Chikungunya virus nonstructural protein 1 as an antiviral target

Kovacikova, K.

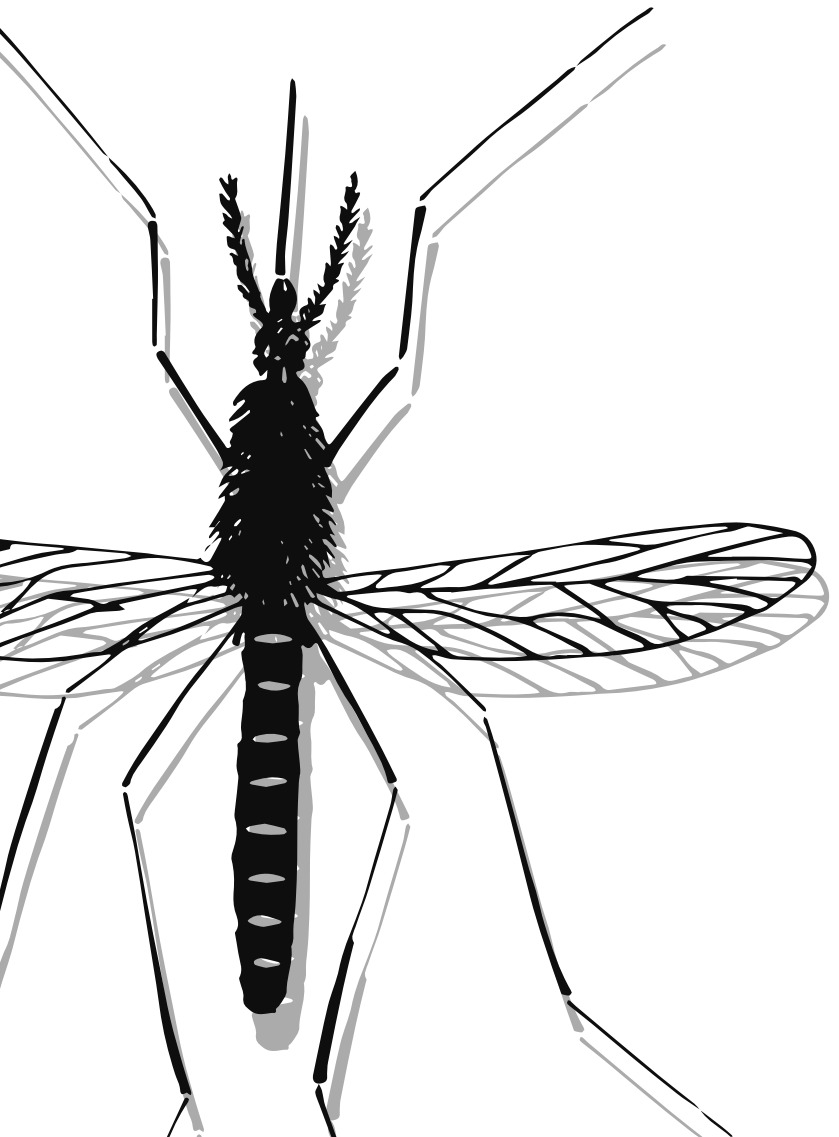

CHAPTER 6

Structural insights into the mechanisms of action of functionally distinct classes of Chikungunya virus nonstructural protein 1 inhibitors

Kristina Kovacikova[a], Marina Gorostiola González[b, c], Rhian Jones[d], Juan Reguera[d], Alba Gigante[e], María-Jesús Pérez-Pérez[e], Gerhard Pürstinger[f], Julia Moesslacher[g], Thierry Langer[h], Lak Shin Jeong[i], Leen Delang[j], Johan Neyts[j], Eric J Snijder[a], Gerard J P van Westen[b] and Martijn J van Hemert[a]

[a] Department of Medical Microbiology, Leiden University Medical Center, Leiden, the Netherlands

[b] Division of Drug Discovery and Safety, Leiden Academic Centre for Drug Research, Leiden University, Leiden, the Netherlands

[c] Oncode Institute, Leiden, the Netherlands

[d] Aix-Marseille Université, INSERM, CNRS, AFMB UMR 7257, Marseille, France

[e] Instituto de Química Médica (IQM-CSIC), Juan de la Cierva 3, E-28006, Madrid, Spain

[f] Department of Pharmaceutical Chemistry, University of Innsbruck, Innsbruck, Austria

[g] Department of Pharmacy, University of Innsbruck, 6020 Innsbruck, Austria

[h] Department of Pharmaceutical Chemistry, University of Vienna, Vienna, Austria

[i] College of Pharmacy, Seoul National University, Seoul, South Korea

[j] KU Leuven, Department of Microbiology, Immunology and Transplantation, Rega Institute for Medical Research, Laboratory of Virology and hemotherapy, Leuven, Belgium

Submitted to AAC

Abstract

Chikungunya virus (CHIKV) nonstructural protein 1 (nsP1) harbours the methyltransferase (MTase) and guanylyltransferase (GTase) activities needed for viral RNA capping and represents a promising antiviral drug target. We compared the antiviral efficacy of nsP1 inhibitors belonging to the MADTP, CHVB and FHNA series [6'-fluoro-homoneplanocin A (FHNA), its 3'-keto form and 6'-β-Fluoro-homoaristeromycin]. Cell-based phenotypic cross-resistance assays revealed that the CHVB and MADTP series shared a similar mode of action that differed from that of the FHNA series. In biochemical assays with purified Semliki Forest virus nsP1, CHVB compounds strongly inhibited MTase and GTase activities, while MADTP-372 and the 3'-keto form of FHNA had only a moderate inhibitory effect. The first of its kind molecular docking studies with the cryo-EM structure of CHIKV nsP1, which is assembled into a dodecameric ring, revealed that the MADTP and CHVB series bind at the SAM-binding site in the capping domain, where they would function as (non) competitive inhibitors. The FHNA series was predicted to bind at the secondary binding pocket in the Ring-Aperture Membrane-Binding and Oligomerization domain, potentially interfering with membrane binding and oligomerization of nsP1. Our cell-based and enzymatic assays, in combination with molecular docking and mapping of compound-resistance mutations to the nsP1 structure allowed us to group nsP1 inhibitors into functionally distinct classes. This study identified druggable pockets in the nsP1 dodecameric structure and provides a basis for rational design, optimization and combination of inhibitors of this unique antiviral drug target.

Introduction

Chikungunya virus (CHIKV) and Semliki Forest virus (SFV) are Old World alphaviruses belonging to the *Togaviridae* family. This group includes mosquito-borne enveloped viruses with single-stranded, positive-sense RNA genomes of approximately 12 kb. CHIKV is an arthritogenic alphavirus transmitted by the *Aedes aegypti* and *Aedes albopictus* mosquitoes. Infections with Old World alphaviruses such as CHIKV typically result in symptoms like fever, rash and polyarthritis/polyarthralgia. In roughly two thirds of the cases, a CHIKV infection progresses into a severe form of persistent debilitating joint paint with long-term sequelae (1). Since its re-emergence in Kenya in 2004, CHIKV has infected millions of people worldwide following its introduction into new territories in Asia, the Caribbean, the Americas and southern Europe (2). Despite recent advances in CHIKV vaccine development (3), prophylactic and/or therapeutic treatment for CHIKV infection is still lacking.

Alphavirus nonstructural proteins (nsPs) are released from a polyprotein precursor by proteolytic cleavage and are indispensable in the alphaviral life cycle (4). The viral replication complex, formed by nsP1-4, assembles in intracellular compartments, termed spherules, which are derived from the host plasma membrane (5, 6). NsP1 is responsible for membrane association of the replication complex (7, 8). In addition, nsP1 catalyses the viral RNA capping, whereby the 5' end of the nascent RNA is modified by attachment of a cap-0 (m^7GpppA) structure. Capping of alphavirus RNA is an essential step in the replication cycle as the cap structure protects viral mRNA from cellular exonucleases, enables its efficient translation and prevents recognition by the host innate immune system. Alphaviruses use a mechanism of mRNA capping that is distinct from that of the host cell. While cellular capping enzymes methylate GTP after it has been transferred to the 5' end of the RNA, alphavirus nsP1 first methylates GTP, after which the methylated GTP (m^7GTP) is covalently attached onto nsP1 and subsequently transferred to RNA (9). In the first step of the alphaviral capping reaction sequence, S-adenosylmethionine (SAM)-dependent N7-methyltransferase (MTase) methylates a GTP molecule while releasing S-adenosylhomocysteine (SAH) as a by-product (10, 11). In the second step, the guanylyltransferase (GTase) activity of nsP1 mediates the attachment of m^7GTP to nsP1 to form the covalent intermediate m^7GMP-nsP1 with release of pyrophosphate (PPi) (12). In the final reaction step, m^7GMP is transferred onto the modified 5' end of the viral mRNAs. Preceding this event, the RNA 5' triphosphatase activity of nsP2

removes the 5'-terminal γ-phosphate from triphosphorylated viral RNAs to yield 5' diphosphate RNAs that can serve as substrate for the m^7GMP transfer from m^7GMP-nsP1, resulting in the formation of a cap-0 structure (13). Early sequence analyses predicted that the N-terminal domain of alphavirus nsP1 [approximately 200 amino acids (aa)] contains a Rossmann fold with conserved sequence motifs, referred to as the 'Core' region, and harbours the MTase activity (14). Later predictions suggested that the putative alphavirus MTase-GTase domain corresponds to the 'Core' region and a C-terminal extension from aa 250 to approximately aa 406, termed the 'Iceberg' region (15). Enzymatic assays with truncated SFV nsP1 indicated that the first 500 aa are required for full enzymatic activity (16). Despite knowledge obtained from mutagenesis studies with recombinant SFV nsP1, the binding sites for the endogenous ligands SAM and GTP are currently not known. A SINV nsP1 mutant resistant to low intracellular GTP levels harbours three mutations in nsP1, namely glutamine-21-lysine (Q21K), serine-23-asparagine (S23N) and valine-302-methionine (V302M) (17), indicating that a potential GTP-binding site might include residues from both the N-terminal and the 'Iceberg' regions of the protein. Furthermore, it is known that specific mutations and deletions within the MTase-GTase domain of alphavirus nsP1 abolish enzymatic activity and yield non-viable viruses (16, 18). For example, the SFV nsP1 aspartic acid-64-alanine (D64A) mutant was unable to bind SAM in a UV cross-linking assay and this mutation interfered with its MTase activity. Furthermore, the SFV nsP1 histidine-38-alanine (H38A) mutation selectively destroyed the GTase activity, presumably by abolishing the covalent attachment of m^7GMP to nsP1 (16). Besides mutational analysis, little progress has been made with regard to understanding and characterizing alphavirus nsP1 functional domains due to the lack of a crystal structure that could provide insight into the spatial organization of various functional residues.

Several CHIKV nsP1 inhibitors have been discovered in recent years (reviewed in (19)), which indicates that alphavirus nsP1 is a promising antiviral drug target. MADTP-372 is a compound belonging to the 3-aryl-[1,2,3]triazolo[4,5-d]pyrimidin-7(6H)-ones or MADTP series (20). Resistance selection and genotyping showed that a proline-34-serine (P34S) substitution in the N-terminal part of CHIKV nsP1 results in resistance to MADTP compounds (21). A threonine-246-alanine (T246A) substitution was also identified as a MADTP resistance mutation (unpublished). 6'-β-Fluoro-homoaristeromycin (FHA) and 6'-fluoro-homoneplanocin A (FHNA) are carbocyclic adenosine analogues with potent anti-CHIKV activity, originally designed as S-adenosylhomocysteine (SAH) hydrolase inhibitors (22). CHIKV mutants carrying

the glycine-230-arginine (G230R) and lysine-299-glutamic acid (K299E) substitutions in nsP1 are resistant to these compounds (22). CHVB-032 and CHVB-066 belong to 2-(4(phenylsulfonyl)piperazine-1-yl)pyrimidine analogues, also known as the CHVB series (23). Selection of resistant variants and reverse genetics studies indicated that (primarily) the combined serine-454-glycine (S454G) and tryptophan-456-arginine (W456R) substitutions in the C-terminal part of CHIKV nsP1 are responsible for CHVB resistance (24). Sinefungin is a SAM analogue that inhibits Venezuelan Equine Encephalitis virus (VEEV) and CHIKV nsP1 in enzymatic assays measuring either MTase or GTase activity (25-27). Besides sinefungin, MADTP-372 and CHVB-066 have also been shown to inhibit the GTase activity of VEEV nsP1 in enzymatic assays (21, 24). We have previously shown that CHVB compounds completely block *in vitro* activity of SFV nsP1 in a covalent m^7GMP-nsP1 complex formation assay (24) and we now report a similar, although less potent, effect for the MADTP series.

Here, we set out to explore the cross-functional relationships between the various CHIKV nsP1 inhibitors (Fig. 1). We aimed to investigate whether these compounds share a similar mechanism of action, by, for example, sharing a binding pocket, and whether this could be linked to a function, e.g. interfering with SAM- or GTP-binding site. To this end, we compared the inhibitors in cell-based cross-resistance assays, enzymatic assays and performed molecular docking on the recently solved CHIKV nsP1 cryo-EM structure (28).

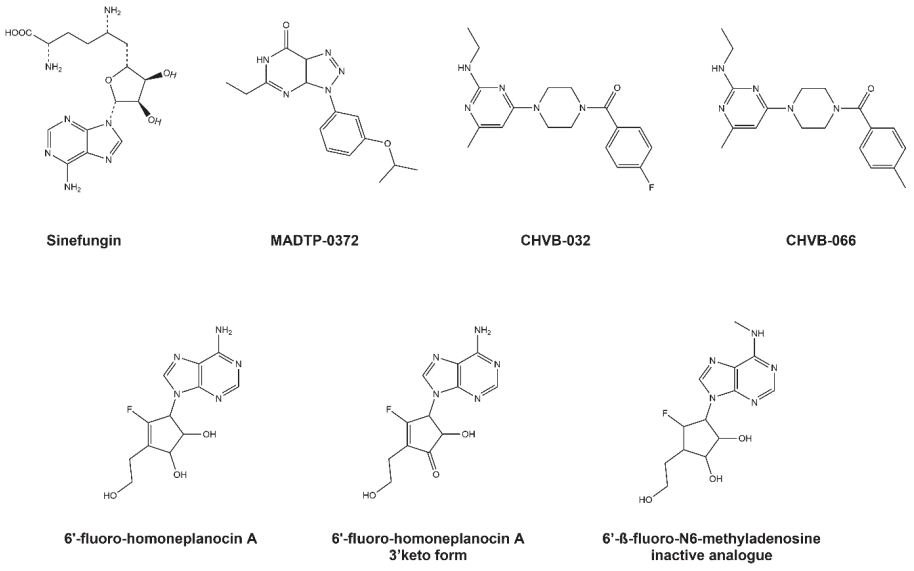

Figure 1: Chemical structures of the CHIKV nsP1-targeting compounds used in this study.

Materials and Methods

Cells and virus strains

VeroE6 cells were grown in Dulbecco's Modified Eagle Medium (DMEM) supplemented with 8% fetal calf serum (FCS) and penicillin/streptomycin. Infection assays were performed in Eagle's Minimum Essential Medium (EMEM) supplemented with 2% FCS, 2 mM L-glutamine and penicillin/streptomycin. CHIKV LS3 (CHIKV, GenBank KC149888) is an infectious clone-derived virus (29). CHIKV nsP1-P34S is a reverse-engineered LS3-derived mutant that is resistant to MADTP compounds (21). CHIKV nsP1-G230R+K299E is a reverse-engineered LS3-derived mutant resistant to FHA and FHNA (22). CHIKV nsP1-S454G+W456R is a reverse-engineered LS3-derived mutant resistant to CHVB-032 and CHVB-066 (24). Semliki Forest virus (SFV) strain SFV4 was used in cytopathic effect (CPE) reduction assays to assess the antiviral spectrum of nsP1 inhibitors.

Compounds

FHA, FHNA and 6'-β-fluoro-N^6-methyladenosine (FMA) were synthesized as described elsewhere (30). The compounds were maintained as 20 mM stock in DMSO at 4°C and used as described before (22). MADTP-372 was synthesized as described elsewhere (20) and 10 mM stock solutions in DMSO were prepared and used as described before (21). Sinefungin (Sanbio) was dissolved to 50 mM in MiliQ. Favipiravir (BOC Sciences) was dissolved to 100 mM in DMSO. CHVB-032 and CHVB-066 were synthesized as described elsewhere (23). CHVB-066 (25.4 mM) and CHVB-032 (29.1 mM) stock solutions in DMSO were prepared and used as described (24). All compounds except FHA, FHNA and FMA were stored at-20°C.

CPE reduction assay

CPE reduction assays were performed as described previously (22). In short, VeroE6 cells were seeded in 96-well clusters at a density of 5 x 10^3 cells/well in DMEM supplemented with 8% FCS. The next day, the cells were incubated with serial dilutions of compounds prepared in EMEM supplemented with 2% FCS and infected with 50 µl/well of CHIKV (MOI 0.005) or SFV (MOI 0.025) or left uninfected. For phenotypic cross-resistance assays, a 10 times higher MOI was used (0.05; 500 PFU/well). The SFV- and CHIKV-infected plates were incubated for 32 h and 96 h, respectively. Cell viability was measured using the MTS/PMS method (Promega, The Netherlands) by

adding 20 µl/well of MTS reagent. The cells were incubated for 2 h followed by fixation with 30 µl/well of 37% formaldehyde. Absorption was measured at 490 nm using an Envision Plate Reader (Perkin Elmer, US). The 50% effective concentration (EC_{50}), defined as the concentration of compound required to inhibit virus-induced cell death by 50%, and the 50% cytotoxic concentration (CC_{50}), defined as the concentration of compound that reduced the cell viability to 50% of that of untreated control cells, were determined using non-linear regression with GraphPad Prism v8.0.

m^7GMP-nsP1 covalent complex formation assay

The covalent m^7GMP-nsP1 complex formation assay was performed as described previously (22). Briefly, the activity of SFV nsP1 was measured in a standard 30 µl reaction containing 25 mM HEPES pH 7.5, 5 mM DTT, 10 mM KCl, 2 mM $MgCl_2$, 100 µM SAM, 0.75 mCi of [α^{32}P] GTP (3000 Ci/mmol) and 0.5 µM wild-type (wt) SFV nsP1 or active site mutant D64A. The reaction was incubated at 30˚C for 30 min and stopped by adding 3 µl of 10% SDS. The reaction mixtures were mixed with 4x Laemmli Sample Buffer (LSB) and then 10 µl samples were separated in a 10% SDS-PAGE gel. The dried gels were placed in a cassette with a PhosphoImager screen. After overnight exposure, the ^{32}P-labelled covalent m^7GMP-nsP1 intermediate products were visualized with a Typhoon Imager (Amersham).

System preparation and CHIKV nsP1 molecular docking

Docking was performed using ICM Pro software, version 3.9-1b (Molsoft LLC, San Diego) (31, 32). The apo CHIKV nsP1 cryo-EM structure representing a dodecameric ring (PDB 6Z0V) was prepared by adding and optimizing the position of hydrogen atoms, as well as the orientation and protonation states of histidine and cysteine residues, and the orientation of glutamine and asparagine residues. ‘Chain A’ in the cryo-EM structure was used as the main nsP1 monomeric structure (referred to as n), and chains n+1 and n-1, flanking chain n, were considered to acknowledge the complexed nature of active nsP1. The binding pockets of endogenous ligands, GTP and SAM, were defined using their corresponding binding pocket residues as proposed by Jones *et al* (28). Both ligands were docked separately using default settings without constraints. Potential small-molecule binding pockets were identified using the ICM Pocket Finder method (33, 34), using chains n and n-1 as a starting point. Two predicted pockets, surrounded by 33 and 18 residues, respectively, were selected based on mutagenesis data. The proposed inhibitors CHVB-066, CHVB-032, MADTP-372, sinefungin, FHNA, 3’-keto

form of FHNA, and FMA were docked into the defined binding pockets with default settings and 10 poses stored for each of them. All ligands were routinely prepared by adding hydrogen atoms and assigning atomic charges. The docking results were analysed in light of the available experimental data, and docking poses were selected accordingly between the top two poses based on docking score and interaction networks.

Results

Cross-resistance analysis of CHIKV nsP1 mutants resistant to different nsP1-targeting compounds

The anti-CHIKV activity of a variety of nsP1-targeting compounds, i.e. CHVB-032, CHVB-066, MADTP-372, FHA, FHNA and sinefungin, was compared in a multi-cycle CPE-reduction assay on VeroE6 cells (Table 1). FHA and CHVB-066 were the most potent compounds with EC_{50} values below 1 µM. FHNA, CHVB-032 and MADTP-372 inhibited CHIKV with EC_{50} in the low micromolar range (1.2 - 3.4 µM). Sinefungin was not a potent inhibitor of CHIKV replication in cell culture, as its EC_{50} was 184.9 µM. None of the compounds was cytotoxic at the effective concentrations. Furthermore, the same compounds were tested against SFV in the same type of multi-cycle infection assay. Interestingly, only FHA and FHNA inhibited SFV replication with EC_{50} values in the low micromolar range (3.9 - 5.2 µM), while the rest of the compounds did not exhibit any antiviral effect against SFV.

Table 1: The antiviral activity of nsP1 inhibitors on CHIKV and SFV replication in CPE reduction assays.

Virus	CHIKV		SFV	
Compound	EC_{50} (µM)[a]	CC_{50} (µM)[b]	EC_{50} (µM)	CC_{50} (µM)
FHA	0.7 ± 0.08	> 250	3.9 ± 3.5	> 250
FHNA	1.2 ± 0.03	> 250	5.2 ± 3.2	> 250
CHVB-066	0.6 ± 0.1	25	NA[c]	25
CHVB-032	3.4 ± 0.3	> 100	NA	> 100
MADTP-372	2.7 ± 0.2	> 100	NA	> 100
sinefungin	184.9 ± 38.4	> 1,000	NA	> 1,000

[a]EC_{50}, concentration of compound that reduces virus-induced CPE by 50%
[b]CC_{50}, concentration of compound that reduces cell viability by 50%
[c]Not active

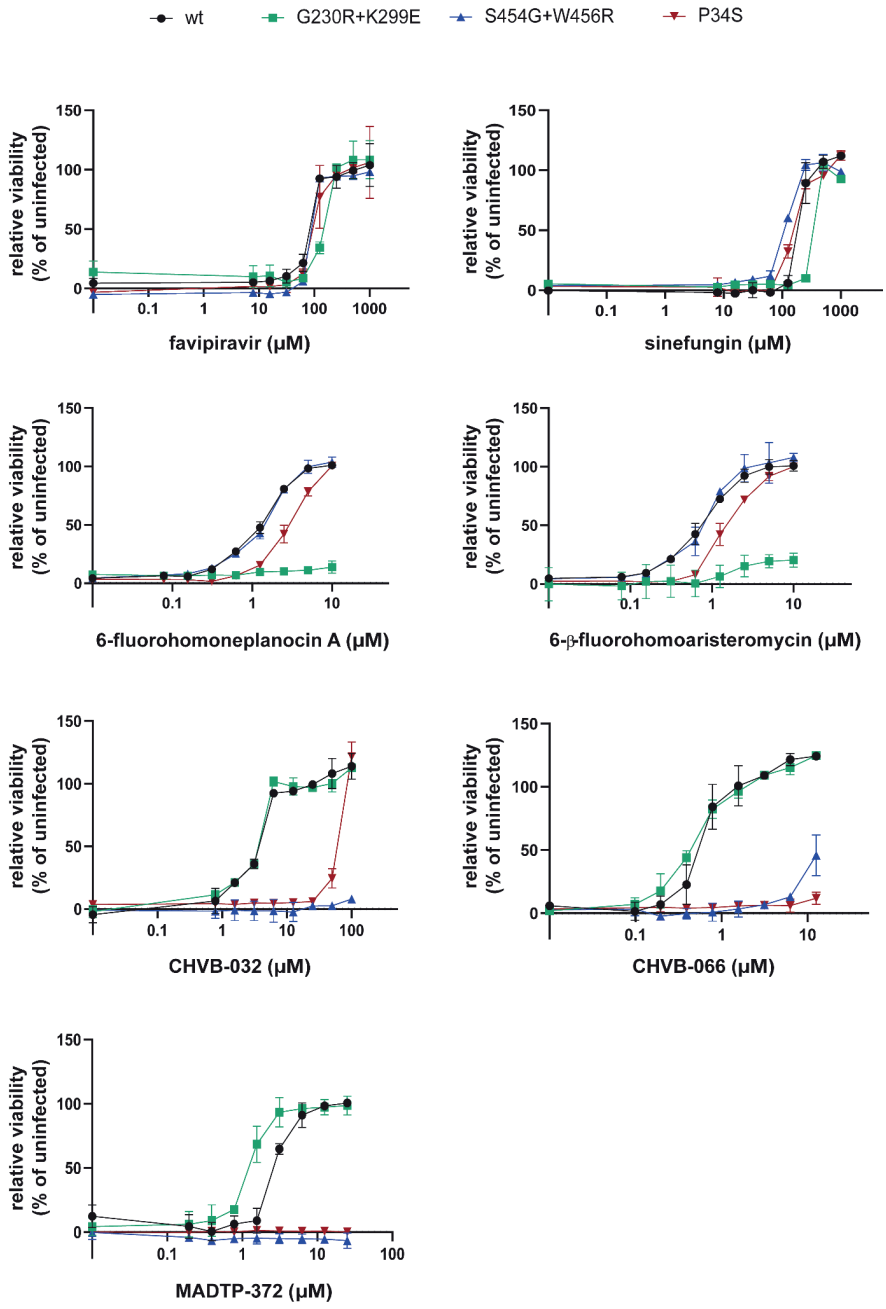

Figure 2: Cross-resistance analysis of compound-resistant CHIKV strains with mutations in nsP1. The sensitivity of wt CHIKV and mutants nsP1-G230R+K299E, nsP1-S454G+W456R and nsP1-P34S towards various nsP1-targeting inhibitors was assessed in CPE reduction assays in VeroE6 cells. The mechanistically unrelated compound favipiravir, which targets nsP4, was included as a control.

Table 2: Resistance and cross-resistance of CHIKV nsP1 compound-resistant mutants nsP1-G230R+K299E, nsP1-S454G+W456R and nsP1-P34S against CHIKV nsP1 inhibitors and against a mechanistically unrelated compound favipiravir.

		rCHIKV P34S		rCHIKV G230R + K299E		rCHIKV S454G + W456R	
Compound	**wt**	**EC_{50} (μM)**	**Fold resistance[a]**	**EC_{50} (μM)**	**Fold resistance**	**EC_{50} (μM)**	**Fold resistance**
FHA	0.7 ± 0.08	1.6 ± 0.2	2.3	> 10	14.3	0.7 ± 0.08	1
FHNA	1.2 ± 0.03	2.8 ± 0.3	2.4	> 10	8.6	1.2 ± 0.1	1
CHVB-066	0.6 ± 0.1	> 12.5	20.8	0.3 ± 0.04	< 1	> 12.5	20.8
CHVB-032	3.4 ± 0.3	52.4 ± 0.8	14.4	3.4 ± 0.2	1	> 100	29.4
MADTP-372	2.7 ± 0.2	> 25	9.3	1.2 ± 0.2	< 1	> 25	9.3
sinefungin	184.9 ± 38.4	150.8 ± 2.5	< 1	274.5 ± 0.2	1.5	109.8 ± 3.9	< 1
favipiravir	79.8 ±1.4	95.9 ± 12.8	1.2	135 ± 5	1.7	89.5 ± 0.2	1.1

[a]Fold resistance = EC_{50} variant/EC_{50} wt

Next, the CHIKV nsP1 mutant carrying the P34S substitution (resistant to MADTP-372) (21), the CHIKV nsP1 mutant carrying the G230R and K299E substitutions (resistant to FHA and FHNA) (22) and, the CHIKV nsP1 mutant carrying the S454G and W456R substitutions (resistant to CHVB-032 and CHVB-066) (24), were tested in cross-resistance phenotypic assays in all possible compound-virus combinations and against the unrelated compound favipiravir (Fig. 2). All resistant mutants were sensitive to favipiravir, a nucleoside analogue that inhibits the CHIKV nsP4 RNA-dependent RNA polymerase (35), and sinefungin, a SAM analogue. CHIKV nsP1-P34S, which was originally selected as a MADTP-resistant virus, was completely resistant to MADTP-372 and to CHVB-066 at the tested concentrations, and it was > 14-fold more resistant to CHVB-032 than wt virus (Fig. 2). Furthermore, CHIKV nsP1-S454G+W456R, originally identified as CHVB-resistant virus, was completely resistant to CHVB-032 and also cross-resistant to MADTP-372 at the tested doses, and to a lesser extent to CHVB-066 (Fig. 2). This suggested that the compounds of the CHVB and MADTP series share a similar mechanism of action. CHIKV nsP1-G230R+K299E was resistant to FHA and FHNA but was sensitive to the CHVB and MADTP series (Fig. 2), suggesting a different mechanism of action that is unrelated to that of the CHVB and MADTP series.

The comparison of fold resistance values, determined as the ratio of the EC_{50} values of the resistant and wt CHIKV, for each resistant mutant-compound combination is included in Table 2.

Inhibition of SFV nsP1 enzymatic activity by nsP1-targeting compounds

We next determined the inhibitory effect of sinefungin, MADTP-372, CHVB-032 and CHVB-066 in an enzymatic assay with purified wt SFV nsP1 that monitors the formation of the covalent m^7GMP-nsP1 complex. This assay measures both MTase and GTase activities and uses the formation of a radioactive ^{32}P-m^7GMP-nsP1 as a readout (22). The active site mutant D64A was used as a negative control as it is devoid of MTase activity (16). CHVB-032 and its analogue CHVB-066 completely blocked the formation of the ^{32}P-m^7GMP-nsP1 covalent complex, as published previously (24). MADTP-372 also inhibited the formation of the ^{32}P-m^7GMP-nsP1 covalent intermediate, but less effectively, as some radioactive signal was still detected even at a 1 mM dose of compound. Sinefungin, on the other hand, was a very inefficient inhibitor, given a slight and steady reduction of signal across the tested concentration range (50 µM to 1 mM) (Fig. 3A). Sinefungin appeared to stimulate GTase activity, as some product was formed in reactions lacking SAM, but containing 50 µM sinefungin (Fig. 3B). This might explain why sinefungin was inactive in a CPE-reduction assay with SFV and exhibited a high EC_{50} value in an assay with CHIKV (Table 1). FHNA (not shown) inhibited the formation of the ^{32}P-m^7GMP-nsP1 covalent intermediate to a lesser extent in a modified assay lacking DTT (22). The 3'-keto form of FHNA, which is suspected to be the active form of the molecule (22), could unfortunately not be tested because we were unable to synthesize this molecule. The combined data from the cell-based cross-resistance analysis and enzymatic assays with purified wt SFV nsP1 suggested that the various compounds can be divided into distinct classes based on their mode of actions. Therefore, we set out to perform molecular docking studies with the individual nsP1 inhibitors and the CHIKV nsP1 cryo-EM structure, in order to understand the structural basis of nsP1 inhibition and to obtain more insights into the potential mechanisms of action of these compounds at the molecular level.

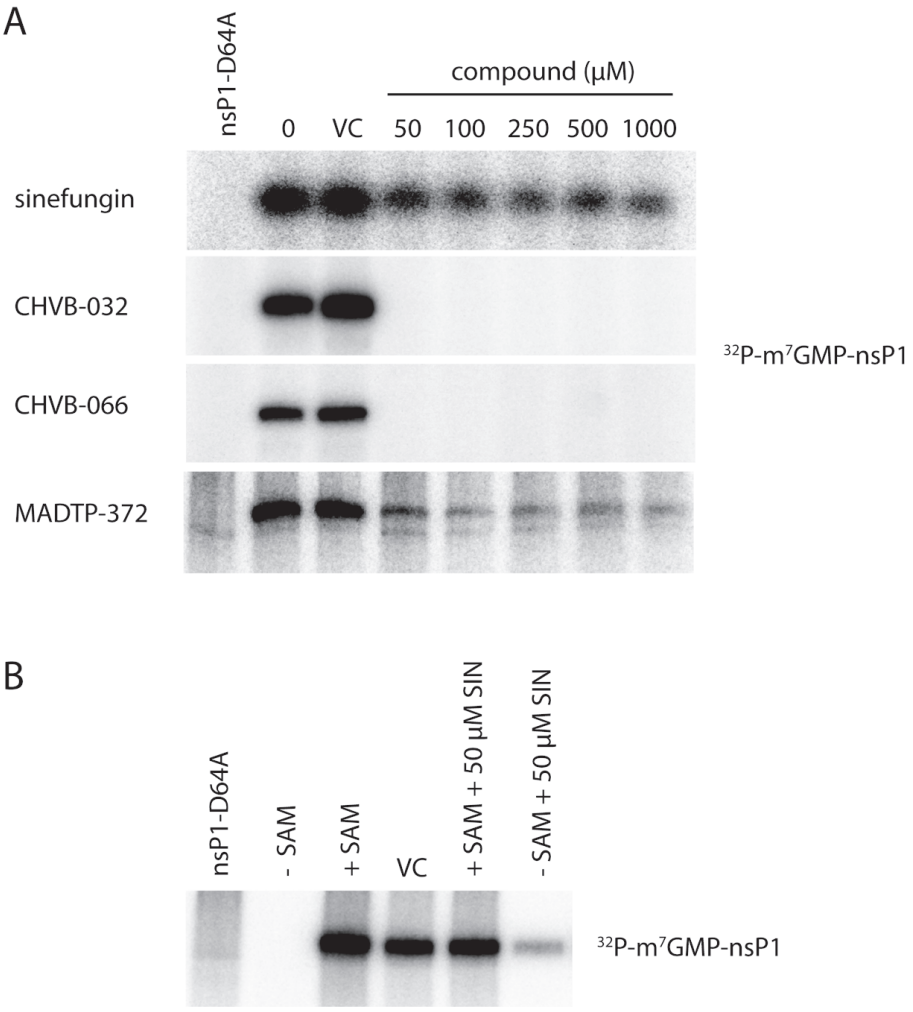

Figure 3: Inhibitory effect of selected compounds on the enzymatic activity of purified wt SFV nsP1 in a biochemical assay that measures the formation of the covalent ^{32}P-m^{7}GMP-nsP1 reaction intermediate. (A) wt SFV nsP1 was incubated with α ^{32}P-GTP and 100 μM SAM and treated with increasing doses (50 μM to 1 mM) of inhibitors. SFV nsP1 D64A was used as a negative control. VC – DMSO-treated control. (B) wt SFV nsP1 was incubated with α ^{32}P-GTP with or without 50 μM sinefungin (SIN) and in the presence or absence of 100 μM SAM. SFV nsP1 D64A was used as a negative control. VC- DMSO-treated control.

Predicted CHIKV nsP1 binding pockets and poses of endogenous ligands

Using the ICM Pocket Finder method (33, 34) and the available CHIKV nsP1 cryo-EM structure representing a dodecameric ring (Fig. 4A and 4B), we identified an elongated ligand binding site, referred to as pocket 1 or the main binding pocket, which is depicted in Fig. 4.

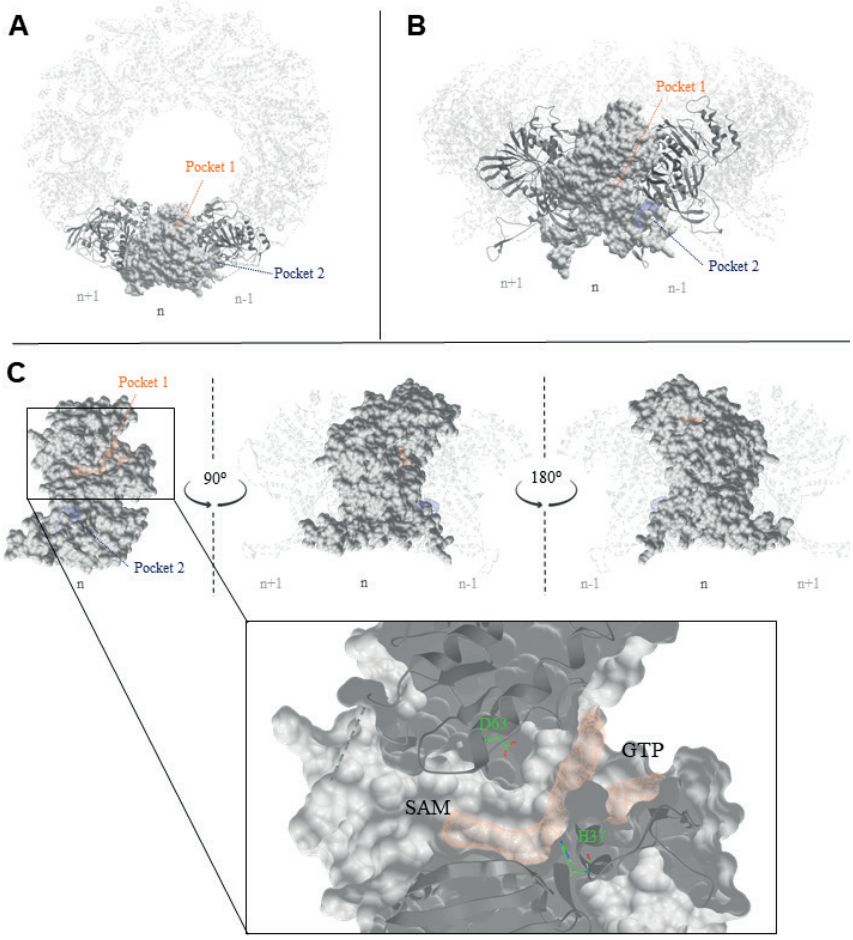

Figure 4: The predicted binding pockets in the CHIKV nsP1 oligomeric structure. (A) Top view of the nsP1 dodecameric ring. Predicted main binding pocket (pocket 1, in orange) and secondary binding pocket (pocket 2, in blue) by the ICM Pocket Finder method. (B) Front view of the nsP1 dodecameric ring. (C) The predicted main binding pocket is elongated and contains two binding sites virtually divided by the catalytic residues H37 and D63, that correspond to the SAM- and GTP-binding sites. Three consecutive nsP1 protomers with subscripts n, n+1 and n-1 were used to define these pockets within the nsP1 complex (PDB 6Z0V).

This pocket is part of the capping domain of nsP1 carrying out the MTase and GTase functions. We further recognized two binding sites in this predicted main binding pocket, which are virtually separated by H37 and D63, and correspond to the GTP- and SAM-binding sites, as defined previously (28). A secondary binding pocket, referred to as pocket 2 in Fig. 4, was identified in the Ring-Aperture Membrane-Binding and Oligomerization (RAMBO) domain of nsP1 involved in membrane binding and oligomerization of nsP1 protomers (28). Based on secondary structure predictions and cross-linking studies with recombinant SFV nsP1 (16), the catalytic site of CHIKV nsP1 is most likely flanked by H37 and D63. The endogenous ligands, GTP and SAM, are expected to bind in the proximity of these residues, as depicted in Fig. 5. However, in the available apo CHIKV nsP1 cryo-EM structure, the D63 residue, which is thought to be the anchor point for SAM (16), is too deeply buried in the protein structure to be accessible to endogenous ligands in docking simulations. Residue H37 is part of the catalytic loop in the active site, defined as a four aa region between residues P34 and H37. We hypothesize that a conformational change takes place during the capping reactions, which increases the solvent exposure of H37 and D63. The proposed GTP-SAM binding mode, depicted in Fig. 5, serves as a reference point in the docking analysis of the various inhibitors in the main binding pocket.

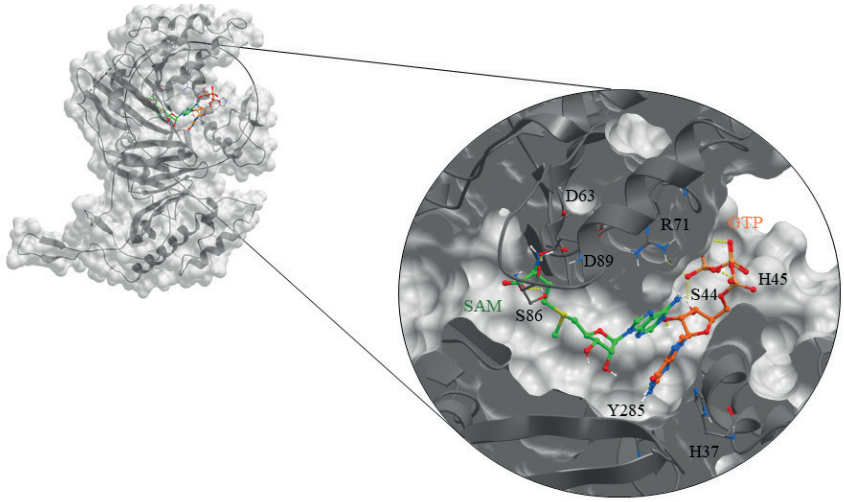

Figure 5: Suggested binding mode of the endogenous ligands, GTP (orange) and SAM (green), in the catalytic pocket of CHIKV nsP1 (grey) generated by molecular docking. Known catalytic residues H37 and D63 are not directly involved in binding, most likely due to the available conformation of the CHIKV nsP1 cryo-EM structure (PDB 6Z0V), where D63 is deeply buried in the protein structure.

Mapping of resistance mutations on the nsP1 structure

Our cross-resistance studies with CHIKV nsP1 mutants revealed a pattern for drug resistance to various CHIKV nsP1-targeting compounds. Namely, the MADTP and CHVB series appear to share a similar mode of action while FHNA and its 3'-keto form (further referred to as the FHNA series) appear to interfere with the CHIKV nsP1 function via a different mechanism. Fig. 6 shows the positions of the aa changes responsible for resistance to these inhibitors on a graphical representation of three consecutive nsP1 protomers as part of nsP1 dodecameric ring (28). The subscripts n+1, n and n-1 refer to the nsP1 protomer to which each aa residue belongs. Residue $P34_n$, the mutation of which causes resistance to the MADTP series, is part of the catalytic loop in the active site and delimits the GTP-binding site. Residues $G230_n$ and $K299_n$, which are mutated in FHNA-resistant virus, are found in different functional regions of nsP1. Residue $G230_n$ is located in the membrane binding and oligomerization (MBO) loop 1 that folds over the n-1 protomer. Residue $K299_n$ lines the entrance to the SAM-binding site of the n+1 protomer. Residues $G230_n$ and $K299_{n-1}$ flank a smaller predicted binding pocket (pocket 2 in Fig. 4) that could explain the mode of action of the FHNA

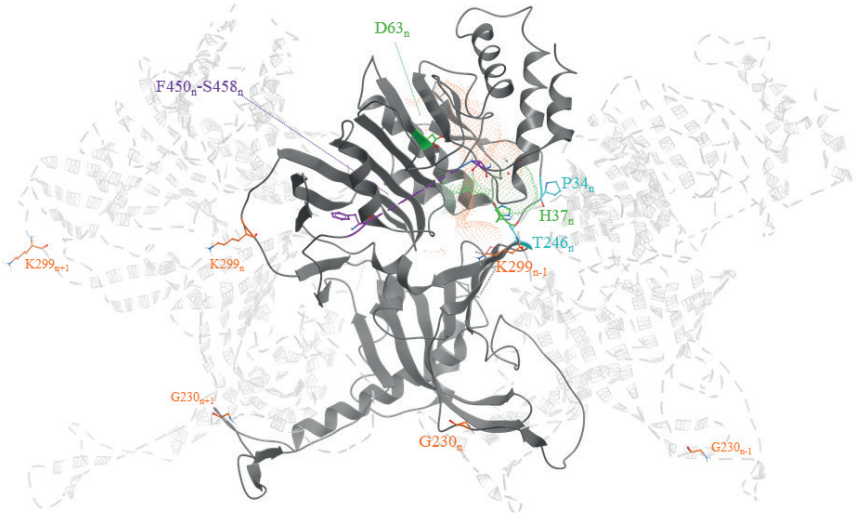

Figure 6: Key amino acid residues linked to drug resistance to CHIKV nsP1 inhibitors mapped to the CHIKV nsP1 cryo-EM structure (PDB 6Z0V) represented as three consecutive nsP1 protomers n, n+1 and n-1. In green, the catalytic residues H37 and D63. In blue, residues P34 and T246, involved in drug resistance to the MADTP series. In orange, residues G230 and K299, conferring drug resistance to the FHNA series. In purple, residues F450 to S458 flank the area where residues S454 and W456, involved in drug resistance to the CHVB series, would be located. Orange and green dotted volumes represent the proposed binding pockets of GTP and SAM, respectively, for reference.

series and the mechanism of drug resistance. Unfortunately, the CHIKV nsP1 cryo-EM structure includes a density gap between residues 450-458 and, therefore, the position of residues S454 and W456, which are mutated in the CHVB-resistant virus, could not be mapped. Presumably, both $S454_n$ and $W456_n$ are located in the proximity of the entrance to the SAM-binding site, based on the position of aa flanking this region.

Predicted binding mode of CHIKV nsP1-targeting compounds

Docking studies with the CHIKV nsP1 cryo-EM structure predicted that compounds of the CHVB and MADTP series bind at the SAM-binding site of `the main binding pocket (Fig. 7A and 7B). In this model, hydrogen bonds with the backbone of Y154 and A155 seem crucial for ligand binding of both series of compounds. Compounds of the CHVB series (CHVB-032 and CHVB-066) are predicted to bind more strongly compared to MADTP-372 (i.e. with lower docking scores) (Table 3). In mutagenesis experiments, it was observed that the mutations P34S and, to a lesser extent, T246A are involved in drug resistance to MADTP-372. Both residues form part of the catalytic site of nsP1 while only P34 is located in the catalytic loop (Fig. 6). Considering the predicted binding poses of MADTP-372 and CHVB compounds, they are unlikely to make direct interactions with P34 or T246, since the distance to these residues is too large. However, residues P34 and, to a lesser extent, T246 appear to be crucial for maintaining the conformation of the catalytic loop in the active site, and their mutations are likely to affect the activity of any small molecule binding at the main binding pocket. The S454G and W456R substitutions, which confer drug resistance to the compounds of the CHVB series, could not be directly mapped in the available cryo-EM structure, but they are likely positioned at the entrance of the SAM-binding site (Fig. 6). Mutations in this region of nsP1 could arise due to a compensatory effect increasing SAM binding or SAM access to the SAM-binding site. Consequently, compensatory mutations would counteract the inhibition by CHVB compounds. The SAM analogue sinefungin was also docked at the predicted main binding pocket, but its pose is not considered here, since it was expected to bind in a similar way as SAM. Based on the docking results presented in Table 3, it could be that sinefungin preferentially drifts to the GTP-binding site because it is more solvent-exposed compared to the SAM-binding site in the current CHIKV nsP1 conformation. The docking results for the FHNA series support the hypothesis that they target a different region and function of nsP1, as

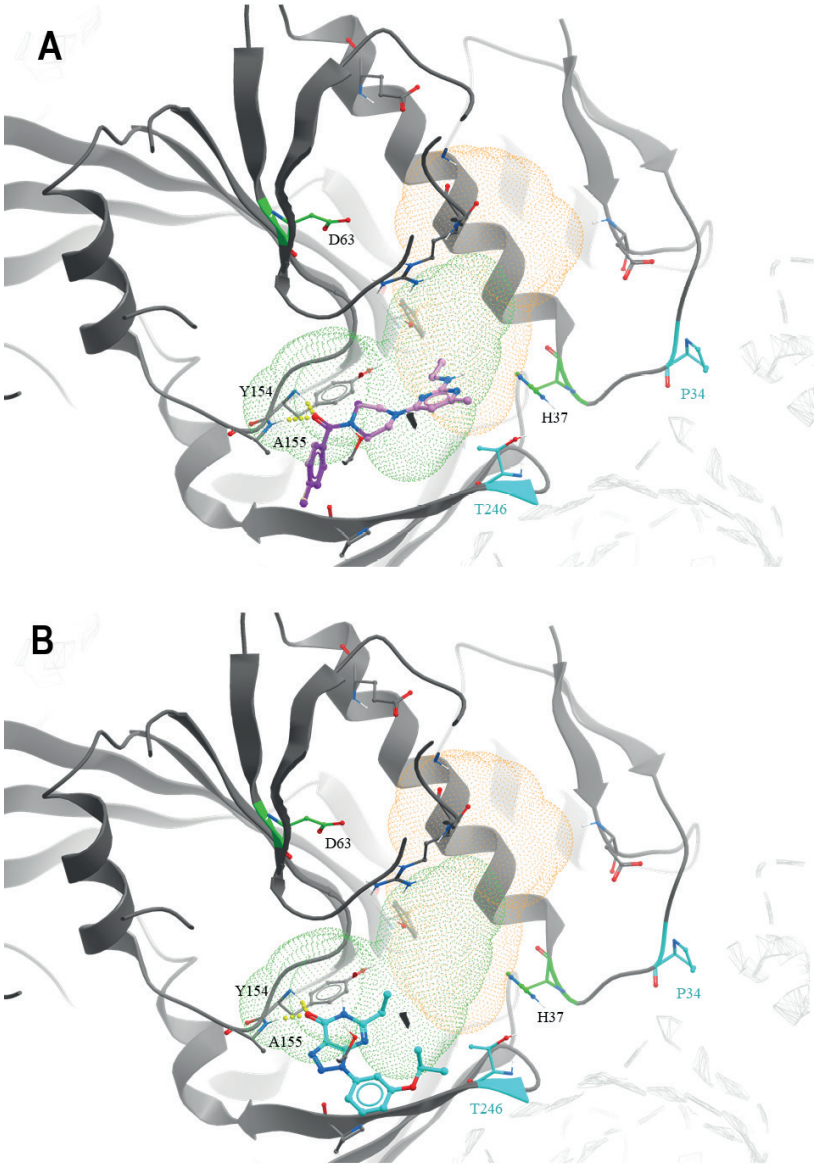

Figure 7: Predicted binding mode of the CHVB and MADTP series in the CHIKV nsP1 SAM-binding site of the main binding pocket (PDB 6Z0V). (A) CHVB-066 (purple) and CHVB-032 (pink) in complex with CHIKV nsP1, occupying the SAM-binding site (green dots). Both CHVB compounds form hydrogen bonds with Y154 and A155 (in yellow) and share a common binding mode. The strength of hydrogen bonds is represented by the diameter of the sphere. (B) MADTP-372 (blue) in complex with CHIKV nsP1, occupying the SAM-binding site (green dots). This compound forms hydrogen bonds with Y154 and A155 (in yellow). P34 (in blue) is the main residue responsible for MADTP compound resistance. T246 (in blue) is an additional residue that upon mutation causes some level of resistance to MADTP.

Table 3: Docking results for selected poses from the ICM small molecule docking method in the main binding pocket (pocket 1) for the endogenous ligands, GTP and SAM, and inhibitors belonging to the CHVB, MADTP, and FHNA series.

Compound	Pocket [a]	Pose	Score [b]	Hbond [c]	Hphob [c]	VwInt [c]
GTP	GTP	1	-33.68	-19.15	-3.27	-31.4
SAM	SAM	1	-2.65	-7.75	-5.30	-21.55
Sinefungin	1 (GTP)	1	-17.35	-11.13	-4.862	-22.55
CHVB-066	1 (SAM)	1	-21.76	-5.051	-7.936	-22.71
CHVB-032	1 (SAM)	1	-21.29	-5.124	-7.414	-21.72
MADTP-372	1 (SAM)	1	-17.54	-5.711	-6.509	-22.21
FHNA	1 (GTP)	2	-14.15	-6.059	-4.099	-21.66
3'-keto form of FHNA	1 (GTP)	1	-13.88	-7.497	-3.73	-18.34
FMA	1 (GTP)	1	-14.97	-6.949	-4.094	-21.27

[a] SAM and GTP in brackets refer to the SAM- and GTP-binding sites, respectively, within the main binding pocket (pocket 1).
[b] Not comparable between different binding pockets.
[c] Hbond, Hphob and VwInt, contribution of the hydrogen bond, hydrophobic, and van der Waals interaction networks to the docking score.

Table 4: Docking results for selected poses from the ICM small molecule docking method in the secondary binding pocket (pocket 2) for inhibitors belonging to the CHVB, MADTP, and FHNA series.

Compound	Pocket	Pose	Score [a]	Hbond [b]	Hphob [b]	VwInt [b]
Sinefungin	2	1	-8.302	-10.93	-4.45	-23.17
CHVB-066	2	1	-6.819	-0.685	-6.887	-24.27
CHVB-032	2	1	-16.51	-3.084	-5.966	-24.1
MADTP-372	2	1	-9.269	-2.374	-4.28	-22.88
FHNA	2	1	-10.26	-4.138	-3.471	-19.22
3'-keto form of FHNA	2	2	-11.25	-8.237	-3.701	-21.76
FMA	2	1	-10.36	-5.363	-3.548	-15.02

[a] Not comparable between different binding pockets.
[b] Hbond, Hphob and VwInt, contribution of the hydrogen bond, hydrophobic, and van der Waals interaction networks to the docking score.

they preferably bind to pocket 2 in the RAMBO domain of nsP1 (Fig. 8A). In pocket 2, the compounds of the FHNA series would form hydrogen bonds with residues close to residue G230, which is involved in drug resistance to this series (Fig. 8B). The inactive analogue FMA could also be docked in pocket 2, but it portrayed a different binding mode, providing a structural basis for the differences in antiviral activity between FHNA and the inactive analogue. In general, the CHVB and MADTP

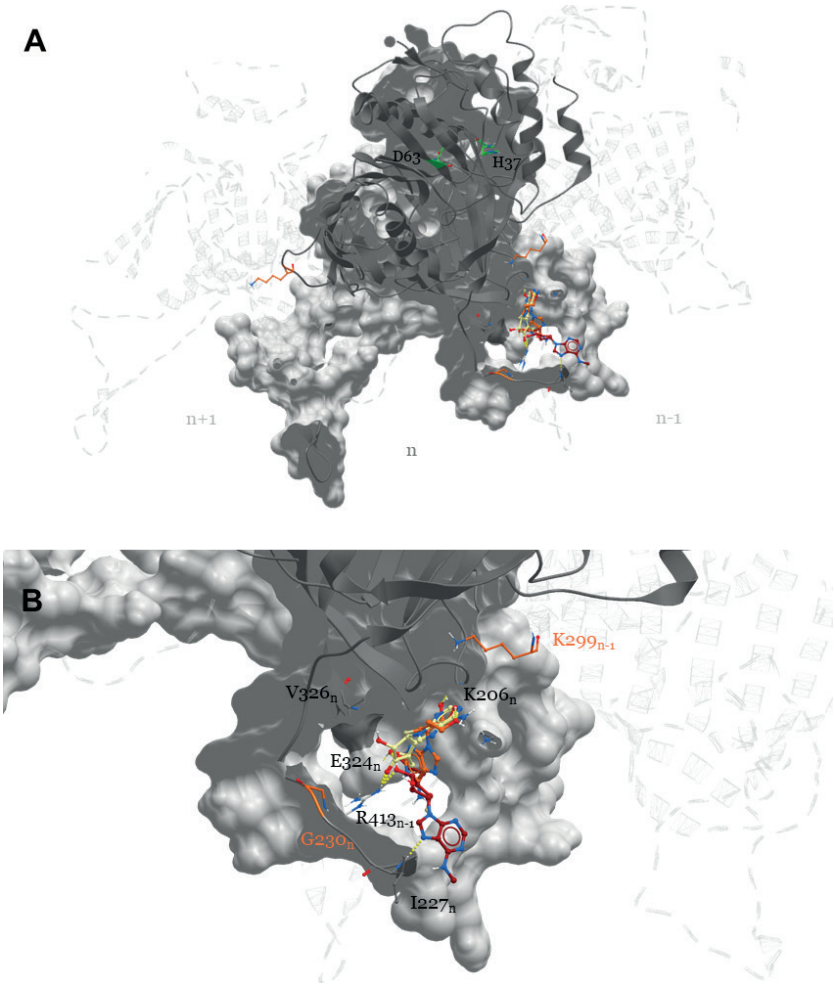

Figure 8: Binding mode of the FHNA series in the CHIKV nsP1 secondary binding pocket. (A) The FHNA series is suggested to bind to a secondary binding pocket (pocket 2) in the RAMBO domain of CHIKV nsP1 (PDB 6Z0V) outside of the main binding pocket. (B) The defined binding pocket is flanked by residues $G230_n$ and $K299_{n-1}$. FHNA and FHA share a similar binding mode that is not shared by the inactive analogue FMA.

series bind with lower affinity to pocket 2 (Table 4), with the exception of CHVB-032, which seems to be stabilized both by hydrogen bonds and hydrophobic interactions in this pocket. The difference between the docking scores of CHVB-066 and CHVB-032 could explain the higher potency of CHVB-066 in anti-CHIKV assays (Table 1), whereby CHVB-032 could be more easily sequestered in pocket 2 compared to its analogue CHVB-066.

Discussion

In this study we have explored the cross-functional relationships of a variety of chemically distinct CHIKV nsP1 inhibitors (Fig. 1). Here, we present a model that could explain the antiviral mechanisms of the inhibitors belonging to the MADTP, CHVB and FHNA series. Cell-based phenotypic cross-resistance assays revealed that the CHVB and MADTP series shared a similar mode of action that differs from that of the FHNA series. Interestingly, all of the CHIKV nsP1 mutants that were resistant to the different nsP1-targeting compounds were sensitive to sinefungin (Fig. 2). In enzymatic assays with wt SFV nsP1, CHVB-032 and CHVB-066 completely blocked the formation of the ^{32}P-m^{7}GMP-nsP1 covalent complex while MADTP-372 also inhibited enzymatic activity, although less potently (Fig. 3A). Sinefungin only weakly inhibited the enzymatic activity and, curiously, its addition to the assay in the absence of SAM led to the formation of a radioactive product, presumably the ^{32}P-m^{7}GMP-nsP1 covalent complex (Fig. 3A and 3B). Both the cell-based and enzymatic assays indicated that these CHIKV nsP1 inhibitors target different functions of the protein. To elucidate the mechanism of action of these compounds in more detail, we performed a molecular docking study with the recently solved CHIKV nsP1 cryo-EM structure. Importantly, the molecular docking experiments described here were performed on an enzymatically active form of CHIKV nsP1. Recently, Jones *et. al.* described that CHIKV nsP1 is active when assembled as oligomers into a ring-shaped membrane-associated complex (28). Using this structure, we identified two binding pockets within a single nsP1 protomer: the main binding pocket (pocket 1) in the capping domain, and the secondary binding pocket (pocket 2) in the RAMBO domain (Fig. 4). The main binding pocket, which forms the catalytic site of CHIKV nsP1, is further divided into two binding sites occupied by the endogenous ligands SAM and GTP (Fig. 5). The mutations responsible for drug resistance to the MADTP, CHVB and FHNA series mapped to different functional regions of CHIKV nsP1 (Fig. 6), supporting our observations from the cell-based and enzymatic assays. The molecular docking experiments predicted that the MADTP and CHVB series bind at the SAM-binding site in the main binding pocket (Fig. 7A and 7B). Here, the MADTP and CHVB compounds would likely exert their inhibitory effect by competing with SAM. The differences in potency of these compounds are supported by differences in docking scores. In contrast, the compounds of the FHNA series most probably bind to a different region of nsP1, seemingly not directly disrupting the catalytic activity (Fig. 8). Instead, the FHNA series appears to interfere with membrane

binding and oligomerization of nsP1 by binding to pocket 2 in the RAMBO domain, and thus indirectly affecting the nsP1 enzymatic function. Lastly, sinefungin does not seem to bind in a similar way to the inhibitors of the MADTP, CHVB and FHNA series. Despite the fact that sinefungin structurally resembles SAM, it preferentially docked at the GTP-binding site (Table 3). However, the docking results for sinefungin need to be interpreted with caution because the SAM's binding pose in itself is not very reliable in the current CHIKV nsP1 conformation. As mentioned in the Materials and Methods, SAM and sinefungin were docked differently (i.e. using different docking grids or reference residues). In addition, more experimental data would need to be obtained to explain why sinefungin stimulates GTase activity and does not serve as a competitive SAM inhibitor. In summary, we identified several classes of CHIKV nsP1 inhibitors with unique modes of action by our cell-based and biochemical assays as well as molecular docking studies.

Furthermore, the molecular docking experiments revealed interesting observations regarding the structural impact of the mutated residues in the MADTP-, CHVB- and FHNA-resistant viruses. The residues conferring resistance to the MADTP and CHVB series were found to gate the SAM-binding site in the main binding pocket (Fig. 6). Specifically, the residues that are mutated in the MADTP-resistant viruses (substitutions P34S and T246A) were located in close proximity to the catalytic residue H37. The residues that are mutated in the CHVB-resistant viruses (substitutions S454G and W456R) were predicted to be located in the proximity to the SAM-binding site despite a density gap in the CHIKV nsP1 structure, which precluded precise mapping of these residues (Fig. 6). Given the predicted position of these aa, both MADTP and CHVB compounds are unlikely to directly interact with these residues in the active site. The observed drug resistance could be achieved by compensatory mutations that destabilize the active site, e.g. the MADTP resistance mutation P34S could affect the position of the catalytic loop in the active site, including the position of the catalytic residue H37. The ensuing conformational change of the active site could thus negatively influence the binding mode of the MADTP series. The same negative effect would be expected to occur by mutating other residues in the catalytic loop, for example, by altering the charge of residue D36. The CHVB resistance mutations also appear to be compensatory as they are predicted to be located further away from the SAM-binding site. These mutations could facilitate SAM binding or increase SAM access to the SAM-binding site. On the contrary, residues $G230_{n}$ and $K299_{n-1}$, which are mutated in the FHNA-resistant virus, flank pocket 2 in the RAMBO domain (Fig. 6).

Residue G230 is located in the MBO loop 1 involved in the formation of membrane-binding spikes, facilitating membrane binding and assembly of oligomeric nsP1. More specifically, residue $G230_n$ promotes interactions with the RAMBO MBO loop 2 of the n-1 protomer. Residue $K299_n$ gates the entry to the SAM-binding site of the n+1 protomer. Interestingly, the V326M substitution, which together with G230R, was previously implicated in resistance to difluoromethylornithine (36), also mapped to pocket 2, suggesting that compounds linked to inhibition of methionine metabolism localize to a discrete binding site within the nsP1 structure (Fig. 8). Furthermore, nsP1 oligomerization allosterically activates the enzyme, therefore, mutations that disrupt this process are expected to lead to a loss of nsP1 enzymatic activity (28). Our enzymatic assays with wt SFV nsP1 revealed that the 3'-keto form of FHNA only partially inhibited the formation of the ^{32}P-m^{7}GMP-nsP1 covalent intermediate (22). The rather negligible inhibitory effect of the 3'-keto form of FHNA in the covalent complex formation assay in comparison with compounds belonging to the MADTP and CHVB series could be explained by its allosteric effect on the nsP1 enzymatic activity, affecting oligomerization of nsP1. Last but not least, FMA, which was inactive in CHIKV CPE-reduction assays, showed a different binding mode compared to active FHNA, which differ by the N-methylation at the N6 position of the purine ring and the double bond on the cyclohexyl ring.

The major limitation of this study and the current model is that the available CHIKV nsP1 cryo-EM structure has no ligands in the active site. In addition, the findings by Jones *et al.* suggest a complex mechanism of nsP1 oligomerization and activation (28), which would be very difficult to capture with the techniques used in this study, potentially leading to discrepancies between the modelled and experimental data. Importantly, the molecular docking experiments presented in this study were performed on the dodecameric form of CHIKV nsP1, which could lead to a potential bias when docking compounds on the monomeric nsP1. For example, MADTP-372 preferentially binds at the GTP-binding site when docked to the monomeric nsP1 as opposed to the oligomeric nsP1. Here, we reported on molecular docking of CHIKV nsP1 inhibitors considering the whole CHIKV nsP1 complex, as we aimed to approximate our results to the active form of CHIKV nsP1 likely found in CHIKV-infected cells, as suggested by Flock House virus tomographic reconstructions of infected cells (28). Furthermore, the resistance mutations described in this study were not located in the compound docking sites in the apo nsP1 structure. Their position might further change upon conformational reorganization of nsP1, which is predicted

to occur after m^7GTP relocates in the proximity of the catalytic residue H37 in the main binding pocket to form the covalent intermediate m^7GMP-nsP1 (28). Previous studies using recombinant SFV or VEEV nsP1 mutants expressed in *E. coli* defined residues important for the catalytic activity of alphavirus nsP1. For example, SFV nsP1 mutants carrying aa substitutions of conserved residues are either completely inactive in assays measuring both MTase and GTase activity (D64A, D90A and C142A) or had a very low level of activity (C135A and Y249A) (16), suggesting an important role of these residues in RNA capping. Using a similar assay, mutational studies with VEEV nsP1 showed that the mutant D63A was devoid of MTase activity while the mutant H37A had abrogated GTase activity (37). All of these residues are positioned at or near the active site in the current CHIKV nsP1 model. Residues H37 and Y248 line the GTP-binding site while residue D89 is exclusively involved in SAM binding. Residues C134 and C141 are found in the Zn binding site below the active site (28). Residue Q19 in VEEV nsP1 was identified as a key residue for the MTase activity, and it was shown that a Q19K mutation modulates SAM and GTP binding (38). This residue was shown to be important for the enzymatic activity of nsP1 and would be expected to lie in the proximity of the active site. Nevertheless, the recent findings by Jones *et al.* describing the process of CHIKV nsP1 oligomerization into structurally novel capping rings challenge the biochemical data from these assays (28). Confirmatory experiments with oligomeric wt and mutant CHIKV nsP1 would need to be performed to validate the results obtained with other forms of alphavirus nsP1. It still remains very puzzling why compounds docking at the active site of CHIKV nsP1, including the MADTP and CHVB series and sinefungin, are not active against a related alphavirus SFV (Table 1). Previously, it was shown that FHA and FHNA, which were active against both CHIKV and SFV, were inactive against SINV (22), and the MADTP and CHVB series were also found to be inactive against other alphaviruses (21, 24). The current opinion in the field holds that the ring-shaped membrane-associated nsP1 complex is conserved among alphaviruses. Besides its enzymatic functions important for RNA capping, the nsP1 complex plays a key role in anchoring the replication complex (nsP1-4) to membranes (4). The nsP1 capping ring appears to interacts with nsP4 on both inner and outer sides of the pore (28).

Taken altogether, this study predicts the mode of action of several CHIKV nsP1 inhibitors. We would like to emphasize that our conclusions are drawn based on a combined interpretation of docking poses and mutagenesis data. Nevertheless, other docking possibilities may exist, especially if different conformations of CHIKV

nsP1 (i.e. other atomic structures in complex with either endogenous or targeted ligands, or monomeric nsP1) would be considered. Our combined data suggest that compounds belonging to the MADTP and CHVB series likely interfere with CHIKV nsP1 functions directly via (non)competitive inhibition of SAM binding. FHNA and its 3'-keto form seem to bind outside of the catalytic site occupied by SAM and GTP and likely have an indirect effect on nsP1 function, possibly by disrupting nsP1 oligomerisation and membrane binding and/or through an allosteric effect on the catalytic site. Since nsP1 oligomerization stabilizes the capping domain, inhibiting this process would compromise the ability of CHIKV nsP1 to perform RNA capping. Our study demonstrates that CHIKV nsP1 is an interesting and relevant antiviral drug target that could be efficiently inhibited by compounds with different mechanisms of action. This would allow development of combination therapy directed at this unique viral activity by combining functionally distinct nsP1 inhibitors and thus lowering the risk of emergence of antiviral drug resistance.

Acknowledgements

K.K. was supported by the Marie Sklodowska-Curie ETN European Training Network "ANTIVIRALS" (EU grant agreement 642434). M.G.G. was supported by funding from the Oncode Institute, the Netherlands. R. J. and J.R. were supported by the ATIP-Avenir program and the Bettencourt Shueller Foundation. M.-J.P.-P. acknowledges the financial support of AEI (PID2019-105117RR-C22).

References

1. Suhrbier A. 2019. Rheumatic manifestations of chikungunya: emerging concepts and interventions. Nat Rev Rheumatol doi:10.1038/s41584-019-0276-9.
2. Burt FJ, Chen W, Miner JJ, Lenschow DJ, Merits A, Schnettler E, Kohl A, Rudd PA, Taylor A, Herrero LJ, Zaid A, Ng LFP, Mahalingam S. 2017. Chikungunya virus: an update on the biology and pathogenesis of this emerging pathogen. Lancet Infect Dis 17:e107-e117.
3. Schrauf S, Tschismarov R, Tauber E, Ramsauer K. 2020. Current Efforts in the Development of Vaccines for the Prevention of Zika and Chikungunya Virus Infections. Front Immunol 11:592.
4. Pietila MK, Hellstrom K, Ahola T. 2017. Alphavirus polymerase and RNA replication. Virus Res doi:10.1016/j.virusres.2017.01.007.
5. Froshauer S, Kartenbeck J, Helenius A. 1988. Alphavirus RNA replicase is located on the cytoplasmic surface of endosomes and lysosomes. J Cell Biol 107:2075-86.
6. Kujala P, Ikaheimonen A, Ehsani N, Vihinen H, Auvinen P, Kaariainen L. 2001. Biogenesis of the Semliki Forest virus RNA replication complex. J Virol 75:3873-84.
7. Lampio A, Kilpelainen I, Pesonen S, Karhi K, Auvinen P, Somerharju P, Kaariainen L. 2000. Membrane binding mechanism of an RNA virus-capping enzyme. J Biol Chem 275:37853-9.
8. Spuul P, Salonen A, Merits A, Jokitalo E, Kaariainen L, Ahola T. 2007. Role of the amphipathic peptide of Semliki forest virus replicase protein nsP1 in membrane association and virus replication. J Virol 81:872-83.
9. Decroly E, Ferron F, Lescar J, Canard B. 2011. Conventional and unconventional mechanisms for capping viral mRNA. Nat Rev Microbiol 10:51-65.
10. Mi S, Stollar V. 1991. Expression of Sindbis virus nsP1 and methyltransferase activity in Escherichia coli. Virology 184:423-7.
11. Laakkonen P, Hyvönen M, Peränen J, Kääriäinen L. 1994. Expression of Semliki Forest virus nsP1-specific methyltransferase in insect cells and in Escherichia coli. J Virol 68:7418-25.
12. Ahola T, Kaariainen L. 1995. Reaction in alphavirus mRNA capping: formation of a covalent complex of nonstructural protein nsP1 with 7-methyl-GMP. Proc Natl Acad Sci U S A 92:507-11.
13. Vasiljeva L, Merits A, Auvinen P, Kaariainen L. 2000. Identification of a novel function of the alphavirus capping apparatus. RNA 5'-triphosphatase activity of Nsp2. J Biol Chem 275:17281-7.
14. Rozanov MN, Koonin EV, Gorbalenya AE. 1992. Conservation of the putative methyltransferase domain: a hallmark of the 'Sindbis-like' supergroup of positive-strand RNA viruses. J Gen Virol 73 (Pt 8):2129-34.
15. Ahola T, Karlin DG. 2015. Sequence analysis reveals a conserved extension in the capping enzyme of the alphavirus supergroup, and a homologous domain in nodaviruses. Biol Direct 10:16.
16. Ahola T, Laakkonen P, Vihinen H, Kaariainen L. 1997. Critical residues of Semliki Forest virus RNA capping enzyme involved in methyltransferase and guanylyltransferase-like activities. J Virol 71:392-7.

17. Scheidel LM, Stollar V. 1991. Mutations that confer resistance to mycophenolic acid and ribavirin on Sindbis virus map to the nonstructural protein nsP1. Virology 181:490-9.
18. Wang HL, O'Rear J, Stollar V. 1996. Mutagenesis of the Sindbis virus nsP1 protein: effects on methyltransferase activity and viral infectivity. Virology 217:527-31.
19. Kovacikova K, van Hemert MJ. 2020. Small molecule inhibitors of Chikungunya virus: mechanisms of action and antiviral drug resistance. Antimicrob Agents Chemother doi:10.1128/aac.01788-20.
20. Gigante A, Canela MD, Delang L, Priego EM, Camarasa MJ, Querat G, Neyts J, Leyssen P, Perez-Perez MJ. 2014. Identification of [1,2,3]Triazolo[4,5-d]pyrimidin-7(6H)-ones as Novel Inhibitors of Chikungunya Virus Replication. J Med Chem 57:4000-8.
21. Delang L, Li C, Tas A, Querat G, Albulescu IC, De Burghgraeve T, Guerrero NA, Gigante A, Piorkowski G, Decroly E, Jochmans D, Canard B, Snijder EJ, Perez-Perez MJ, van Hemert MJ, Coutard B, Leyssen P, Neyts J. 2016. The viral capping enzyme nsP1: a novel target for the inhibition of chikungunya virus infection. Sci Rep 6:31819.
22. Kovacikova K, Morren BM, Tas A, Albulescu IC, van Rijswijk R, Jarhad DB, Shin YS, Jang MH, Kim G, Lee HW, Jeong LS, Snijder EJ, van Hemert MJ. 2020. 6'-beta-Fluoro-Homoaristeromycin and 6'-Fluoro-Homoneplanocin A Are Potent Inhibitors of Chikungunya Virus Replication through Their Direct Effect on Viral Nonstructural Protein 1. Antimicrob Agents Chemother 64.
23. Moesslacher J, Battisti V, Delang L, Neyts J, Abdelnabi R, Pürstinger G, Urban E, Langer T. 2020. Identification of 2-(4-(Phenylsulfonyl)piperazine-1-yl)pyrimidine Analogues as Novel Inhibitors of Chikungunya Virus. ACS Med Chem Lett 11:906-912.
24. Abdelnabi R, Kovacikova K, Moesslacher J, Donckers K, Battisti V, Leyssen P, Langer T, Puerstinger G, Quérat G, Li C, Decroly E, Tas A, Marchand A, Chaltin P, Coutard B, van Hemert M, Neyts J, Delang L. 2020. Novel Class of Chikungunya Virus Small Molecule Inhibitors That Targets the Viral Capping Machinery. Antimicrob Agents Chemother 64.
25. Mudgal R, Mahajan S, Tomar S. 2020. Inhibition of Chikungunya virus by an adenosine analog targeting the SAM-dependent nsP1 methyltransferase. FEBS Lett 594:678-694.
26. Kaur R, Mudgal R, Narwal M, Tomar S. 2018. Development of an ELISA assay for screening inhibitors against divalent metal ion dependent alphavirus capping enzyme. Virus Res 256:209-218.
27. Allison AB, Stallknecht DE, Holmes EC. 2015. Evolutionary genetics and vector adaptation of recombinant viruses of the western equine encephalitis antigenic complex provides new insights into alphavirus diversity and host switching. Virology 474:154-62.
28. Jones R, Bragagnolo G, Arranz R, Reguera J. 2020. Capping pores of alphavirus nsP1 gate membranous viral replication factories. Nature. Accepted for publication.
29. Scholte FE, Tas A, Martina BE, Cordioli P, Narayanan K, Makino S, Snijder EJ, van Hemert MJ. 2013. Characterization of synthetic Chikungunya viruses based on the consensus sequence of recent E1-226V isolates. PLoS One 8:e71047.
30. Chandra G, Moon YW, Lee Y, Jang JY, Song J, Nayak A, Oh K, Mulamoottil VA, Sahu PK, Kim G, Chang TS, Noh M, Lee SK, Choi S, Jeong LS. 2015. Structure-Activity Relationships of Neplanocin A Analogues as S-Adenosylhomocysteine Hydrolase Inhibitors and Their Antiviral and Antitumor Activities. J Med Chem 58:5108-20.

31. Abagyan R, Totrov M, Kuznetsov D. 1994. ICM—A new method for protein modeling and design: Applications to docking and structure prediction from the distorted native conformation. Journal of Computational Chemistry 15:488-506.
32. Neves MA, Totrov M, Abagyan R. 2012. Docking and scoring with ICM: the benchmarking results and strategies for improvement. J Comput Aided Mol Des 26:675-86.
33. An J, Totrov M, Abagyan R. 2004. Comprehensive identification of “druggable” protein ligand binding sites. Genome Inform 15:31-41.
34. An J, Totrov M, Abagyan R. 2005. Pocketome via comprehensive identification and classification of ligand binding envelopes. Mol Cell Proteomics 4:752-61.
35. Delang L, Segura Guerrero N, Tas A, Querat G, Pastorino B, Froeyen M, Dallmeier K, Jochmans D, Herdewijn P, Bello F, Snijder EJ, de Lamballerie X, Martina B, Neyts J, van Hemert MJ, Leyssen P. 2014. Mutations in the chikungunya virus non-structural proteins cause resistance to favipiravir (T-705), a broad-spectrum antiviral. J Antimicrob Chemother 69:2770-84.
36. Mounce BC, Cesaro T, Vlajnic L, Vidina A, Vallet T, Weger-Lucarelli J, Pasoni G, Stapleford KA, Levraud JP, Vignuzzi M. 2017. Chikungunya virus overcomes polyamine depletion by mutation of nsP1 and the opal stop codon to confer enhanced replication and fitness. J Virol doi:10.1128/jvi.00344-17.
37. Heidari Z, Tinsley J, Bickerdike R, McLoughlin MF, Zou J, Martin SA. 2015. Antiviral and metabolic gene expression responses to viral infection in Atlantic salmon (Salmo salar). Fish Shellfish Immunol 42:297-305.
38. Nadia R, Oney OG, Gilles Q, Bruno C, Etienne D, Bruno C. 2020. Mutations on VEEV nsP1 relate RNA capping efficiency to ribavirin susceptibility. Antiviral Res doi:10.1016/j.antiviral.2020.104883:104883.